PHYSICAL REVIEW B **81**, 100505(R) (2010)

Helical instability of charged vortices in layered superconductors

A. Gurevich
National High Magnetic Field Laboratory, Florida State University, Tallahassee, Florida 32310, USA
(Received 13 December 2009; revised manuscript received 12 February 2010; published 9 March 2010)

It is shown that the electric charge of vortices can result in a helical instability of straight vortex lines in layered superconductors, particularly Bi-based cuprates or organic superconductors. This instability may result in a phase transition to a uniformly twisted vortex state, which could be detected by torque magnetometry, neutron diffraction, electromagnetic, or calorimetric measurements.

DOI: 10.1103/PhysRevB.81.100505 PACS number(s): 74.25.Bt, 74.25.Ha, 74.25.Uv, 74.72.−h

Vortices in superconductors carry the quantized magnetic flux $\phi_0=2\times10^{-7}$ Oe cm^2 resulting from the macroscopic phase coherence of superconducting state. Vortices also carry a nonquantized electric charge q caused by the suppression of superconductivity in the vortex core.[1–6] In low-T_c s-wave superconductors this charge is usually negligible and does not manifest itself in the electromagnetic response of vortices driven by the Lorentz force of superconducting currents. However, the situation changes in superconductors with short coherence length ξ, low superfluid density, and unconventional pairing symmetry combined with the competition of superconductivity with nonsuperconducting spin or charged ordered states, as characteristic of high-T_c cuprates, recently discovered oxypnictides or organic superconductors.[7] For cuprates, theoretical estimates[1–4] predict a relatively large fraction $\sim10^{-3}$ of the electron charge e per each pancake vortex residing on the ab planes, yet even larger charge of different sign was observed by nuclear quadrupole resonance.[8] It has been suggested[1] that the vortex charge could change the sign of the Hall coefficient observed in cuprates[9] or result in structural transformations of the vortex lattice.[10]

In this Rapid Communication we show that vortex charge can cause an intrinsic helical instability of a rectilinear vortex and a phase transition to a twisted vortex state. This instability is different from the helical instability of vortices driven by either currents flowing along the vortex line[11] or by screw dislocations[12] or twisted vortex states in rotating liquid He.[13] The buckling instability of vortices results from the Coulomb repulsion of charged pancake vortices which tend to shift away from the straight line along the c axis as illustrated by Fig. 1. Such charge fragmentation is inhibited by the vortex line tension caused by weak magnetic and Josephson coupling of vortex pancakes[14,15] and also by charge screening, which confines the relative displacements of pancakes on neighboring ab planes within the Thomas-Fermi screening length λ_{TF}. Thus, the helical instability would be most pronounced in layered materials with low vortex line tension and $\lambda_{TF}\sim\xi$, as characteristic of high-T_c cuprates, ferropnictides, or organic superconductors.

To calculate properties of spiral vortices we write the excess linear charge $\rho(r)$ in a vortex as follows:

$$\rho(r)=\frac{\rho_0\xi^2}{r^2+\xi^2}+\rho_a\exp(-r^2/2\xi^2). \quad (1)$$

Here the first term is the Ginzburg-Landau (GL) contribution resulting from the change in the chemical potential μ around the core, $\rho_{\rm BCS}(r)\propto[\Delta^2(r)-\Delta_0^2]$, $\Delta(r)\simeq\Delta_0 r/(r^2+\xi^2)^{1/2}$ is the modulus of the order parameter, $\rho_0=eN\Delta_0^2\partial\ \ln T_c/\partial\mu$, and N is the density of states at the Fermi surface in the normal state. The GL vortex charge $q_{\rm BCS}\simeq2\pi\xi^2\rho_0\ln(\lambda/\xi)$ is spread over the London penetration depth λ.[2] Strong dependence of the critical temperature T_c on doping enhances ρ_0 in cuprates. The term $\propto\rho_a$ in Eq. (1) is added phenomenologically to take into account the localized core charge due to competing superconducting and antiferromagnetic orders in unconventional superconductors.[5,6] NMR experiments indicate[8] that the local core charge in cuprates can greatly exceed the BCS contribution. Equation (1) corresponds to the following Fourier transform $\rho(k)=2\pi\xi^2[\rho_0K_0(k\xi)+\rho_a\exp(-k^2\xi^2/2)]$ and the total excess charge per unit length $q\simeq2\pi\xi^2[\rho_0\ln(\lambda/\xi)+\rho_a]$, where $K_0(x)$ is the modified Bessel function.

The excess charge density $\rho(r)$ in a superconductor is screened in the same way as in a normal metal.[1–4] Screening is determined by the Fourier transform of the static dielectric function $\epsilon(\mathbf{k})$, which, for the isotropic Thomas-Fermi model equals $\epsilon(k)=1+\kappa^2/k^2$, where $\kappa=1/\lambda_{TF}$. The Fourier transform of the electric potential $\varphi(k,p)$ produced by a charged curved vortex parameterized by its displacement $\mathbf{u}(z)$ relative to the z axis is given by the Poisson equation:

$$(k^2+p^2)\epsilon(k,p)\varphi(\mathbf{k},p)=4\pi\rho(\mathbf{k})\int_{-\infty}^{\infty}e^{-ipz+i\mathbf{k}\mathbf{u}(z)}dz, \quad (2)$$

where $\epsilon(k,p)$ in a uniaxial material depends on both the in-plane wave vector k and the z component p perpendicular to the layers. From Eq. (2), we obtain the functional of electrostatic energy $W\{\mathbf{u}(z)\}=(1/2)\int\rho\varphi d^3\mathbf{r}$:

$$W=\int\frac{|\rho(k)|^2d^2\mathbf{k}dpdz_1dz_2}{4\pi^2(k^2+p^2)\epsilon(k,p)}e^{ip(z_2-z_1)+i\mathbf{k}[\mathbf{u}(z_1)-\mathbf{u}(z_2)]}. \quad (3)$$

Here two periodic structures $\mathbf{u}(z)$ are considered: helical distortions, $u_x=u\cos Qz$ and $u_y=u\sin Qz$, and planar zigzag distortions, $u_x=u\cos Qz$ and $u_y=0$, where u and Q quantify the amplitude and the period of the structures. For the spiral vortex, we have $\mathbf{ku}(z_1)-\mathbf{ku}(z_2)=2u\sin(Qz_-)[k_x\sin(Qz_+)+k_y\cos(Qz_+)]$, where $z_\pm=(z_1\pm z_2)/2$. Neglecting a possible dependence of $\rho(k,p)$ on p due to charge modulation along the z axis, integrating Eq. (3) over z_1+z_2 and the polar angle in the $\mathbf{k}$ plane, and adding the elastic energy F_e gives the total line energy of a vortex helix $F_s=F_e+W_s$ where

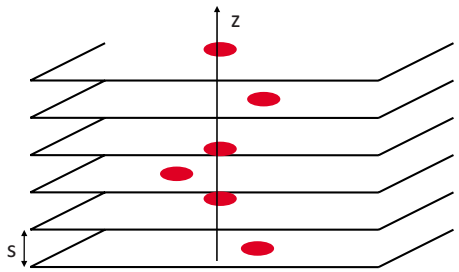

FIG. 1. (Color online) Spiral instability of a straight chain of charged pancake vortices in a layered superconductor.

$$W_s = \int_0^\infty k|\rho(k)|^2 dk \int_{-\infty}^{\infty} dpdz \frac{e^{-2ipz} J_0[2uk|\sin Qz|]}{\pi(k^2+p^2)\epsilon(k,p)}, \quad (4)$$

$$F_e = \frac{u^2\varepsilon_0 Q^2}{4\gamma^2} \ln \frac{\lambda^2\gamma^2}{\xi^2(1+\lambda^2Q^2)} + \frac{\varepsilon_0 u^2}{4\lambda^2} \ln(1+\lambda^2Q^2). \quad (5)$$

Here F_e describes the dispersive tilt energy of a vortex in a uniaxial superconductor,[14,15] $J_0(x)$ is the Bessel function, $\gamma = \lambda_c/\lambda$ is the anisotropy parameter, and $\varepsilon_0 = (\phi_0/4\pi\lambda)^2$ is the vortex energy scale. For a zigzag vortex, we obtain $F_z = F_e/2 + W_z$, where W_z is given by Eq. (4) in which $J_0[2uk|\sin Qz|]$ is replaced by $J_0^2[uk|\sin Qz|]$. To determine which of the two structures has lower energy, we minimize F_s and F_z with respect to u and Q using $\epsilon(k,p)$ for a layered metal:[16]

$$\epsilon(k,p) = \epsilon_0 + \frac{\epsilon_0 s^2\kappa^2 \sinh(ks)}{2[\cosh(ks) - \cos(ps)]sk}, \quad k < 2k_F, \quad (6)$$

where $\kappa^2 = 4\pi^2 e^2\hbar^2/m^*\epsilon_0 s^2$, s is the interlayer spacing, ϵ_0 is the background dielectric constant, m^* is the electron effective mass, and k_F is the Fermi momentum. For $k > 2k_F$, the last factor k in the denominator should be replaced by $k - \sqrt{k^2 - 4k_F^2}$. Equation (6) takes into account the anisotropy of screening at large k and the Friedel oscillations due to singularity in $\partial\epsilon/\partial k$ at $k = 2k_F$. For $(ks, ps) \ll 1$, Eq. (6) reduces to the Thomas-Fermi dielectric function $\epsilon(k,p) = [1 + \kappa^2/(k^2+p^2)]\epsilon_0$ with the screening length $\lambda_{TF} = \kappa^{-1}$.

Now we show that a rectilinear vortex along the c axis becomes unstable with respect to bending distortions if q exceeds a critical line charge q_c. At the instability threshold $q \approx q_c$, Eq. (4) can be expanded in small u, and the z integration produces the δ functions at $k = 0$ and $k = \pm Q$ yielding the following change in W_e:

$$\delta W_s = -\frac{u^2}{2} \int_0^\infty \left[\frac{|\rho(k)|^2 k}{\epsilon(k,0)} - \frac{|\rho(k)|^2 k^3}{(k^2+Q^2)\epsilon(k,Q)} \right] dk. \quad (7)$$

Hence helical distortions do reduce W_e, the electrostatic energy gain increasing as Q increases. The quadratic expansion of Eq. (3) for zigzag distortions yields $\delta W_z = \delta W_s/2$. Given that the charged vortex core is typically larger than either λ_{TF} and s, we expand $\epsilon(k,p)$ in $(ks)^2 \ll 1$ since the integral in Eq. (7) is mostly determined by the region $k^2 \ll \kappa^2$, and $|\rho(k)|^2$ rapidly decreases for $k > \xi^{-1}$. As the result, the energy change for small u takes the form

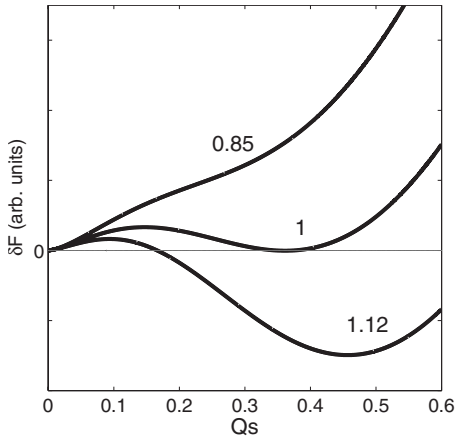

FIG. 2. Energy of the helical vortex line as a function of the wave vector Q and different ratios of q/q_c described by Eq. (8) for $\lambda/s = 10^3$ and $(2\lambda_{TF}/s)^2 = 10$.

$$\delta F_s = F_e - \frac{q^2u^2}{4r_0^4\epsilon_0\kappa^2} \left[1 - \frac{4\sin^2(Qs/2)}{Q^2s^2 + (2Q/\kappa)^2\sin^2(Qs/2)} \right]. \quad (8)$$

Here the effective core radius r_0 is defined by $q^2/2r_0^4 = \int_0^\infty k^3|\rho(k)|^2 dk = 4\pi^2\int_0^\infty (\nabla\rho)^2 r dr$ and Eq. (1), giving $r_0 = \xi$ at $\rho_a \gg \rho_0$. As q exceeds q_c, the function $\delta F_s(Q)$ shown in Fig. 2 first becomes negative at a finite Q. Such behavior reflects the effect of crystalline anisotropy, which strongly reduces the vortex line tension at $Q\lambda \gg 1$ thus facilitating the short wavelength instability. The equation $\partial_Q \delta F_s = 0$ at $Q\lambda \gg 1$ yields

$$Q^2 = \kappa^2/2 \ln(\gamma/\xi Q) \quad (9)$$

so that the twist pitch $\ell_s \simeq 2^{3/2}\pi \ln^{1/2}(\gamma/\xi\kappa)\lambda_{TF} \sim 10\lambda_{TF}$. For $\lambda_{TF} = 0.5-1$ nm in cuprates,[17] $\ell_s \simeq 5-10$ nm turns out to be larger than ξ. From the equation $\delta F(q_c, Q) = 0$ and Eqs. (8) and (9) we obtain the critical charge q_c strongly reduced by crystalline anisotropy:

$$q_c^2 = 2(r_0\kappa)^4\varepsilon_0\epsilon_0[\ln(\gamma/\xi Q) + 1/2]/\gamma^2. \quad (10)$$

Given the relation $\delta F_s = 2\delta F_z$, both helical and zigzag instabilities occur at the same q_c and Q, so to see which of these structures has lower energy, the amplitude of spontaneous distortions u at $q > q_c$ is to be calculated. Near the instability threshold $q \approx q_c$, the general Eq. (4) can be expanded in powers of small u up to terms $\sim u^4$ and integrated at $(r_0\kappa)^2 \gg 1$ as before. This gives the energy change for the spiral vortex: $\delta F_s/F_0 = -\alpha_s u^2 + \beta_s u^4/4$, where $\alpha_s = (1 - q_c^2/q^2)$, $\beta_s = 6Q^2/r_0^2(\kappa^2 + 4Q^2)$, and $F_0 = q^2Q^2/4r_0^2\kappa^2(\kappa^2 + Q^2)\epsilon_0$. Minimization of δF yields the dependence $u(q)$ characteristic of the second-order phase transition:

$$u^2 = \frac{\zeta r_0^2}{3}\left(4 + \frac{\kappa^2}{Q^2}\right)\left(1 - \frac{q_c^2}{q^2}\right)$$

$$\simeq \frac{2\zeta r_0^2}{3}\left(2 + \ln\frac{\gamma}{\xi\kappa}\right)\left(1 - \frac{q_c^2}{q^2}\right), \quad (11)$$

where $\zeta = r_0^2\int_0^\infty |\rho(k)|^2 k^5 dk / \int_0^\infty |\rho(k)|^2 k^3 dk \to 1$ if $\rho_a \gg \rho_0$. For $q \sim q_c$, the amplitude of the vortex helix is of the order of ξ,

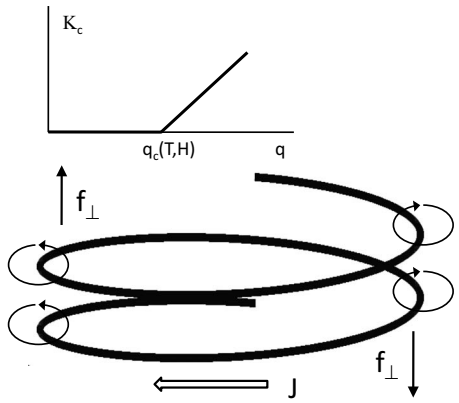

FIG. 3. Mechanism of the torque exerted by a transverse current on the vortex helix where closed lines depict currents circulating around the vortex core. The upper part shows the torque as a function of the line charge $q(T,H)$.

and the total energy gain equals $\delta F_s = -\alpha_s^2 F_0/\beta_s$. For a zigzag vortex, we obtain $\alpha_z = \alpha_s/2$ and $\beta_z = 3\beta_s/8$. Thus, $\delta F_z = 2\delta F_s/3$, so a helical vortex, which provides the maximum spacing between charged vortex pancakes at a given u, is more energetically favorable than a zigzag vortex, which can lower its energy by transverse buckling distortions.

The instability criterion $q > q_c$ depends on T. For example, the BCS vortex charge $q \propto \Delta_0^2 \xi^2$ in Eq. (1) is independent of T at $T_c - T \ll T_c$, while $q_c \propto \varepsilon_0^{1/2} \xi^2 \propto (1 - T/T_c)^{-1/2}$ in Eq. (10) diverges at T_c, suggesting that the helical instability occurs below a certain temperature $T_h < T_c$. However, the NMR experiments[8] show that the observed q is mostly determined by the non-BCS core contribution modeled by the term $\propto \rho_a$ in Eq. (1). Currently little is known about $\rho_a(T)$, so we analyze the criterion $q > q_c$ at low T where it can be expressed in terms of observable parameters. It is convenient to rewrite $q > q_c$ in the form $\eta > \eta_c$ where $\eta_c = qs/e$ is the fraction of the electron charge e per pancake vortex, and

$$\eta_c = \frac{s(r_0\kappa)^2 \epsilon_0^{1/2}}{2^{3/2}\lambda\gamma}\left(\frac{\hbar c}{e^2}\right)\ln^{1/2}\left(\frac{\gamma}{\kappa\xi}\right). \tag{12}$$

For $YBa_2Cu_3O_{\{7-x\}}$ with $\epsilon_0 = 25$, $\lambda_{TF} = 0.5$ nm,[17] $\lambda = 200$ nm, $r_0 = 1.5$ nm, $s = 0.85$ nm, and $\gamma = 5$, Eq. (12) gives $\eta_c \approx 1.6$, much larger than $\eta \sim (0.2–2) \times 10^{-2}$ observed for the optimally doped $YBa_2Cu_3O_7$.[8] Larger values of $\eta \sim (1–5) \times 10^{-2}$ were observed for $YBa_2Cu_3O_8$.[8] The situation becomes more interesting for layered cuprates and organic superconductors, for which $\gamma \sim 100–600$.[7] For Bi-2212 with $s = 1.5$ nm, $\lambda = 200$ nm, $\gamma = 500$, $\epsilon_0 = 10$, and $\kappa r_0 = 3$, we obtain $\eta_c \simeq 4 \times 10^{-2}$ per double CuO planes. Therefore, layered cuprates (particularly underdoped ones) and organic superconductors would be promising candidates for the experimental search for helical vortices, particularly at low T where the vortex core size in the clean limit $r_0(T) \sim \xi(0)T/T_c$ may decrease due to the Kramer-Pesch effect.[18] Such non-GL core shrinkage strongly reduces q_c in Eq. (10) and could result in an unusual case of $r_0(T) < \lambda_{TF}$ for which the instability is further enhanced by stronger Coulomb interaction of pancake vortices.

The single vortex helical instability may result in a long-range twist of the interacting vortex lattice. Indeed, if helical displacements $\mathbf{u}(z)$ of all vortices are phase locked, they do not change the flux density $\nabla \cdot \mathbf{u} = 0$ and thus contribute to neither the shear nor the compression energy of the twisted vortex lattice. Thus, as far as the elastic and electrostatic energies are concerned, vortex structures with a long-range chiral order would be more energetically favorable than structures with different signs of Q or phases of helical distortions on neighboring vortices. In this case the vortex lattice would undergo a phase transition at $q > q(T,B)$ to a uniformly twisted state. Fluctuations and pinning of vortices and proliferation of topological defects may destroy the long range chiral order at higher T and B, however if the spacing between pinning centers is much greater than the twist pitch ℓ, pinning does not affect the single-vortex helical instability. The mean-field phase transition at $q = q_c$ results in the specific heat jump $\Delta C = 2F_0 TB(\partial_T \alpha_s)^2 F_0/\phi_0\beta_s = TB(\kappa^2 + 4Q^2)(\partial_T q - \partial_T q_c)^2/3\phi_0\kappa^2(\kappa^2 + Q^2)\epsilon_0$. If $\partial_T q_c \gg \partial_T q$, we have $\Delta C/\Delta C_0 \sim TB\xi^2 \ln(\gamma/\xi\kappa)/T_c B_{c2}\lambda_{TF}^2\gamma^2\epsilon_0$, where $\Delta C_0 = T_c(\partial_T H_c)^2/8\pi$ is the specific heat jump at T_c.

Interaction of vortices can be taken into account by adding the elastic twist energy $B\phi_0 u^2 Q^2/16\pi(1 + Q^2\lambda^2) \simeq \phi_0 B u^2/16\pi\lambda^2$ (Refs. 14 and 15) in Eq. (5). Then the problem reduces to the helical instability of a single vortex with a field-dependent line tension $\tilde{\varepsilon}_l = (\varepsilon_0/\gamma^2)\ln(\gamma/\xi Q) + \phi_0 B/8\pi\lambda^2 Q^2$, where the last term results from the magnetic cage potential.[14,15] Minimization of $F(Q)$ at $q = q_c$ and $Qs \lesssim 1$ yields

$$Q^4\left(2\ln\frac{\gamma}{\xi Q} - 1\right) = \left(Q^2 + \frac{4\pi B\gamma^2}{\phi_0}\right)\kappa^2, \tag{13}$$

$$q_c^2 = 2\varepsilon_0\epsilon_0 r_0^4\kappa^2(\kappa^2 + Q^2)\left(\frac{1}{\gamma^2}\ln\frac{\gamma}{\xi Q} + \frac{2\pi B}{\phi_0 Q^2}\right). \tag{14}$$

For $B < \phi_0/8\pi\lambda_{TF}^2\gamma^2$, Eqs. (13) and (14) reduce to Eqs. (9) and (10). For $B \gg \phi_0/8\pi\lambda_{TF}^2\gamma^2$, we have $Q \sim (B/\phi_0)^{1/4}(\gamma\kappa)^{1/2}$, which gives the critical charge $q_c \simeq (r_0^2/\lambda\lambda_{TF})(\epsilon_0\phi_0 B/4\pi)^{1/2}$ independent of anisotropy. The instability region $T < T_h(B)$ defined by $q(T_h) > q_c(T_h, B)$ thus widens as B decreases.

Helical distortions with $Q \sim \kappa$ can produce minibands in the spectrum of core quasiparticles moving along the vortex. This may affect the vortex viscosity, vortex mass, and pinning, and also smear the discrete core levels in the scanning tunnel microscope (STM) images of a helical vortex. Vortex chirality also manifests itself in a "fountainlike" currents along the z axis[12,13] and features of flux dynamics controlled by the Lorentz force $\mathbf{f} = (\phi_0/c)[\mathbf{J} \times \mathbf{t}]$ exerted by the current density $\mathbf{J}$ per unit vortex length where $\mathbf{t}(z) = \partial_s \mathbf{r}/|\partial_s \mathbf{r}|$ is a tangent unit vector along the vortex helix parameterized by $\mathbf{r} = (u\cos Qz, u\sin Qz, z)$ and $ds = dz\sqrt{1 + Q^2u^2}$. Transport current distorts the helix, yet the net Lorentz force $\mathbf{F} = (\phi_0/c)\int_0^L [\mathbf{J} \times \mathbf{t}]ds = (\phi_0 L/c)[\mathbf{J} \times \mathbf{z}]$ is independent of chirality. The Lorentz forces acting on a helical vortex also produce the torque $\tau = \int_0^L [\mathbf{r} \times \mathbf{f}]ds/L$ absent for a straight vortex.

Substituting here $\mathbf{f}=(\phi_0/c)[\mathbf{J}\times\mathbf{t}]$, we obtain that the uniform current density $\mathbf{J}_\perp$ perpendicular to the helix produces the net torque per unit length along the z axis

$$\tau=\phi_0 u^2[\mathbf{J}_\perp\times\mathbf{Q}]/2c, \tag{15}$$

as illustrated in Fig. 3. The net torque $\mathbf{K}=\tau BV/\phi_0$ exerted by closed magnetization current loops vanishes, but a uniform current I flowing along a film strip of length L in a perpendicular magnetic field results in the global torque directed along the y axis:

$$K_c=-u^2QBIL/2c. \tag{16}$$

Here $\mathbf{K}_c(q)$ exhibits the behavior characteristic of the second-order phase transition: $K_c=0$ if $q<q_c$ and $K_c\propto 1-(q_c/q)^2$ for $q>q_c$ even for the field H directed along the symmetry axis (see Fig. 3). This distinguishes K_c from the conventional torque $\mathbf{K}_a=[\mathbf{M}\times\mathbf{H}]$ of tilted straight vortices in a uniaxial superconductor for which K_a vanishes at $\mathbf{H}\|c$. To estimate the magnitude of K_c, we compare it with $K_a(\theta)=VH\phi_0(1-\gamma^{-2})\sin 2\theta\ln[\eta H_{c2}/H\varepsilon_\theta]/64\pi^2\lambda^2\varepsilon_\theta$ for $\mathbf{H}$ inclined by the angle θ relative to the c axis where $\varepsilon_\theta=(\cos^2\theta+\gamma^{-2}\sin^2\theta)^{1/2}$.[19] For $uQ\simeq\kappa\xi>1$, we obtain that K_c exceeds K_a at $J\sim J_0\lambda_{TF}/\xi<J_0$ for any θ, where $J_0=c\phi_0/16\pi^2\lambda^2\xi$ is of the order of the depairing current density. Thus, the sensitive torque magnetometry could be used to detect twisted vortex structures.

Helical vortices for $\mathbf{H}$ inclined with respect to the c axis may interfere with the chain and kinked vortex structures in layered superconductors in tilted magnetic fields.[20] Twisted vortex state may also affect the spiral instability caused by longitudinal currents in the Lorentz force free configurations $\mathbf{J}\|\mathbf{H}$,[11] resulting in asymmetry of the c-axis critical currents parallel and antiparallel to the twist pitch. One could also expect manifestations of the helical overdamped soft modes at $q\simeq q_c$ in the Josephson plasma resonance in layered superconductors at $\mathbf{H}\|c$ and the effect of the chiral mixed state on electrodynamics and the magneto-optical Kerr effect.[21]

In conclusion, vortex charge can result in helical vortex instability which can enforce a spontaneous macroscopic twist of the vortex lattice. This can manifest itself in electrodynamic and thermodynamic properties of layered superconductors.

This work was supported by NSF through Grant No. NSF-DMR-0084173 and by the State of Florida.

[1] D. I. Khomskii and A. Freimuth, Phys. Rev. Lett. **75**, 1384 (1995).
[2] G. Blatter, M. Feigelman, V. Geshkenbein, A. Larkin, and A. van Otterlo, Phys. Rev. Lett. **77**, 566 (1996).
[3] J. Kolacek, P. Lipavsky, and E. H. Brandt, Phys. Rev. Lett. **86**, 312 (2001).
[4] T. Koyama, J. Phys. Soc. Jpn. **70**, 2102 (2001); M. Machida and T. Koyama, Physica C **378-381**, 443 (2002).
[5] D. P. Arovas, A. J. Berlinsky, C. Kallin, and S. C. Zhang, Phys. Rev. Lett. **79**, 2871 (1997); Y. Chen, Z. D. Wang, J. X. Zhu, and C. S. Ting, *ibid.* **89**, 217001 (2002); D. F. Agterberg, M. Sigrist, and H. Tsunetsugu, *ibid.* **102**, 207004 (2009).
[6] M. Eschrig and J. A. Sauls, New J. Phys. **11**, 075009 (2009).
[7] J. Singleton and C. Mielke, Contemp. Phys. **43**, 63 (2002); J. S. Brooks, Rep. Prog. Phys. **71**, 126501 (2008).
[8] K. I. Kumagai, K. Nozaki, and Y. Matsuda, Phys. Rev. B **63**, 144502 (2001).
[9] T. Nagaoka, Y. Matsuda, H. Obara, A. Sawa, T. Terashima, I. Chong, M. Takano, and M. Suzuki, Phys. Rev. Lett. **80**, 3594 (1998) and the references therein.
[10] W. Halperin *et al.*, 2009 APS March Meeting (unpublished).
[11] J. R. Clem, Phys. Rev. Lett. **38**, 1425 (1977); E. H. Brandt, Phys. Rev. B **25**, 5756 (1982).
[12] B. I. Ivlev and R. S. Thompson, Phys. Rev. B **44**, 12628(R) (1991).
[13] V. B. Eltsov, A. P. Finne, R. Hanninen, J. Kopu, M. Krusius, M. Tsubota, and E. V. Thuneberg, Phys. Rev. Lett. **96**, 215302 (2006).
[14] G. Blatter, M. V. Feigel'man, V. B. Geshkenbein, A. I. Larkin, and V. M. Vinokur, Rev. Mod. Phys. **66**, 1125 (1994).
[15] E. H. Brandt, Rep. Prog. Phys. **58**, 1465 (1995).
[16] A. L. Fetter, Ann. Phys. **88**, 1 (1974); S. Das Sarma and J. J. Quinn, Phys. Rev. B **25**, 7603 (1982); J. K. Jain and P. B. Allen, Phys. Rev. Lett. **54**, 2437 (1985).
[17] J. Mannhart, Supercond. Sci. Technol. **9**, 49 (1996); C. H. Ahn J.-M. Triscone, and J. Mannhart, Nature (London) **424**, 1015 (2003); A. Rüfenacht, J.-P. Locquet, J. Fompeyrine, D. Caimi, and P. Martinoli, Phys. Rev. Lett. **96**, 227002 (2006).
[18] L. Kramer and W. Pesch, Z. Phys. **269**, 59 (1974).
[19] V. G. Kogan, Phys. Rev. B **24**, 1572 (1981).
[20] A. E. Koshelev, Phys. Rev. B **68**, 094520 (2003); **71**, 174507 (2005).
[21] J. Xia, E. Schemm, G. Deutscher, S. A. Kivelson, D. A. Bonn, W. N. Hardy, R. Liang, W. Siemons, G. Koster, M. M. Fejer, and A. Kapitulnik, Phys. Rev. Lett. **100**, 127002 (2008).